

## SUPPORTING INFORMATION FOR

### **Photoactive carbon monoxide-releasing coordination polymer particles**

Arnau Carné-Sánchez,<sup>\*,a,b</sup> Shuya Ikemura,<sup>a,d</sup> Reiko Sakaguchi,<sup>a</sup> Gavin A. Craig,<sup>\*,a,c</sup> Shuhei Furukawa<sup>\*,a,d</sup>

<sup>a</sup>Institute for Integrated Cell-Material Sciences, Kyoto University, Yoshida, Sakyo-ku, Kyoto 606-8501, Japan

<sup>b</sup>Catalan Institute of Nanoscience and Nanotechnology (ICN2) CSIC and The Barcelona Institute of Science and Technology Campus UAB, Bellaterra, 08193 Barcelona, Spain.

<sup>c</sup>Department of Pure and Applied Chemistry, University of Strathclyde, 295 Cathedral Street, Glasgow, G1 1XL, United Kingdom.

<sup>d</sup>Department of Synthetic Chemistry and Biological Chemistry, Graduate School of Engineering, Kyoto University, Katsura, Nishikyo-ku, Kyoto 615-8510, Japan

[shuhei.furukawa@icems.kyoto-u.ac.jp](mailto:shuhei.furukawa@icems.kyoto-u.ac.jp)

## Contents

<b>Experimental procedures</b>	1
<b>Fig. S1.</b> FT-IR spectra for <b>CORP-1</b> and <b>Model_BIm</b> .	5
<b>Fig. S2.</b> Solid-state UV-vis spectroscopy data for <b>CORP-1</b> and <b>Model_BIm</b> .	6
<b>Fig. S3.</b> PXRD data for <b>CORP-1</b> and <b>CORP-2_small</b> .	7
<b>Fig. S4.</b> Mercury view of a fragment of <b>Model_BIm</b> and PDF data for <b>CORP-1</b> .	8
<b>Fig. S5.</b> IR spectrum of <b>CORP-1</b> , and IR spectrum of <b>CORP-1</b> after being stirred in phosphate buffered saline (PBS) for one day.	9
<b>Fig. S6.</b> IR spectrum of <b>CORP-1</b> , and IR spectrum of <b>CORP-1</b> after irradiation for 2 hours.	10
<b>Fig. S7.</b> Change in the solid-state UV-vis spectra for <b>CORP-1</b> after irradiation.	11
<b>Fig. S8.</b> UV-vis spectra of <b>Model_BIm</b> in MeOH solution.	12
<b>Fig. S9.</b> Customised set-up for in-line detection of CO release.	13
<b>Fig. S10.</b> IR spectra for the large and small particles of <b>CORP-1</b> .	14
<b>Fig. S11.</b> Comparison of the XAFS spectra for the large and small particles of <b>CORP-1</b> .	15
<b>Fig. S12.</b> PDF comparison of <b>CORP-1</b> and <b>CORP-1_small</b> .	16
<b>Fig. S13.</b> IR spectrum of <b>CORP-2</b> , and IR spectrum of <b>Model_BIm</b> for comparison.	17
<b>Fig. S14.</b> Solid-state UV-vis spectroscopy data for <b>CORP-2_small</b> and <b>Model_BIm</b> .	18
<b>Fig. S15.</b> PDF data for <b>CORP-2</b> .	19
<b>Fig. S16.</b> XAFS spectra for <b>CORP-2</b> and <b>Model_BIm</b> .	20

## Experimental procedures

### Synthesis.

MnBr(CO)<sub>5</sub> (Sigma-Aldrich, 98%),  $\alpha,\alpha'$ -dibromo-p-xylene (Wako, 98%), 4,4'-bis(bromomethyl)biphenyl (Wako, 96%), imidazole (Wako, 98%), 2-methylimidazole (Wako, 98%), 1-benzylimidazole (Sigma-Aldrich, 99 %), 1-benzyl-2-methylimidazole (Sigma-Aldrich, 90%), and Rhodamine B (Nacalai Tesque) were purchased from commercial suppliers and used without further purification. The ligand 1,4-bis(imidazol-1-ylmethyl)benzene (Bix) was synthesized according to a reported procedure.<sup>1</sup> The ligand 4,4'-bis(imidazol-1-ylmethyl)biphenyl (bpBix) was synthesized according to the same procedure as the synthesis of Bix.

**[Mn(Bix)<sub>1.5</sub>(CO)<sub>3</sub>]Br (CORP-1).** An acetone solution (4 mL) of MnBr(CO)<sub>5</sub> (40.0 mg, 0.146 mmol) was prepared in a microwave vial and 1.5 mol. equiv. of the ligand Bix (52.0 mg, 0.218 mmol) was added. This mixture was heated at 65 °C for 12 h or kept at room temperature for 24 h. The resulting yellow particles were recovered by centrifugation and washed with acetone three times to remove starting reagents. Finally, the samples were dried under vacuum.

**[Mn(Bix)<sub>1.5</sub>(CO)<sub>3</sub>]Br (CORP-1\_small).** An acetone solution (4 mL) of MnBr(CO)<sub>5</sub> (10.0 mg, 0.036 mmol) was prepared in a microwave vial and 1.5 mol. equiv. of the ligand Bix (13.0 mg, 0.055 mmol) was added. This mixture was heated at 65 °C for 12 h or kept at room temperature for 24 h. The resulting yellow particles were recovered by centrifugation and washed with acetone three times to remove starting reagents. Finally, the samples were dried under vacuum.

**[Mn(bpBix)<sub>1.5</sub>(CO)<sub>3</sub>] (CORP-2\_small).** To an acetone solution (4 mL) of MnBr(CO)<sub>5</sub> (10.0 mg, 0.036 mmol), 1.5 mol. equiv. of the ligand bpBix (17.2 mg, 0.055 mmol) was added. The mixture was heated at 65 °C for 12 h. The resulting yellow particles were recovered by centrifugation and washed with acetone three times. Finally, the samples were dried under vacuum.

**[Mn(BIm)<sub>3</sub>(CO)<sub>3</sub>]Br (Model\_BIm).** In a round bottom flask, MnBr(CO)<sub>5</sub> (178 mg, 0.65 mmol) and 1-benzylimidazole (BIm) (308.5 mg, 1.95 mmol) were dissolved in dichloromethane (35 ml). The solution was stirred at room temperature for 5 h. The solvent was removed under vacuum and the residue was washed three times with tetrahydrofuran. Samples were dried under vacuum to give a yellow solid. Crystals suitable for single crystal X-ray diffraction were obtained by vapour diffusion of diethyl ether into a dichloromethane solution of **Model\_BIm**.

### **Physical characterisation.**

**Powder X-ray diffraction (PXRD)** measurements were performed in Bragg-Brentano geometry using a Rigaku Smartlab (Dtex Ultra detector) operating with a rotating anode Cu K $\alpha$  X-ray generator ( $\lambda = 1.54 \text{ \AA}$ ) with a 45 kV beam voltage and 200 mA current.

**Infrared (IR) spectroscopy** data were recorded on KBr discs using a Jasco FT/IR-6100 with 1  $\text{cm}^{-1}$  resolution and 64 scans.

**UV-visible (UV-vis) spectroscopy** data were recorded using a Jasco V-670 equipped with USE-753 for solution phase measurements or a 60 mm integrated sphere ISN-723 for solid compounds.

**Scanning electron microscopy (SEM)** images were collected using a field-emission scanning electron microscope (JEOL Model JSM-7001F4) operating at 5 kV and 5 mA current.

**Inductively coupled plasma (ICP) spectroscopy** measurements to determine metal ion concentrations were performed in aqueous media using an ICPE-9000 (Shimadzu).

**X-ray Absorption Fine Structure (XAFS) analysis.** The X-ray absorption spectra (XAS) were collected at the beamline BL5S1 at Aichi Synchrotron Radiation Center. The powder samples were mixed with boron nitride with a given amount and ground for 15 minutes and pressed at 1000 kg N for 3 minutes by a standard 7 mm die. XAS in the energy region of the K-edge were measured in transmission mode with a double-crystal monochromator and ion chambers and processed using the IFEFFIT library. Fourier transformation was k<sup>3</sup>-weighted in the k range from 3 to 10  $\text{\AA}^{-1}$ .

**Pair Distribution Function (PDF) analysis.** The X-ray total scattering measurements were performed at SPring-8 on the beamline BL02B2. Samples were sealed in a Lindemann glass capillary. The data were collected at 25  $^{\circ}\text{C}$  using a large Debye–Scherrer camera with an imaging-plate-type detector and imaging plate converting the  $Q (= 4\pi\sin\theta/\lambda)$  range from 0.5 to 20  $\text{\AA}^{-1}$ . The incident beam was monochromated at  $\lambda = 0.35314 - 0.35548 \text{ \AA}$ . The correction of the data for Compton scattering, multiplicative contributions, and Fourier transformation were performed with PDFgetX3.<sup>2</sup> A Gauss window ( $\exp[-BQ^2]$ ,  $B = 0.015$ ) was applied before converting the structure functions into PDFs to suppress truncation errors. The reduced pair distribution function  $G(r)$  is defined as follows:

$$G(r) = 4\pi r \rho_0 \{g(r) - 1\},$$

where  $\rho_0$  is the average number density and  $g(r)$  is the pair distribution function.  $G(r)$  is directly obtained from the Fourier transformation of  $S(Q)$ , and the value of atomic number density is not necessary in  $G(r)$ .

**Single crystal X-ray diffraction (SCXRD)** was performed at 93 K with a Rigaku XtaLab P200 diffractometer and a Dectris Pilatus 200 K CCD system equipped with a MicroMax-007 HF/VariMax rotating-anode X-ray generator with confocal monochromatized Mo K $\alpha$  radiation. Using Olex2,<sup>3</sup> the structure was with the SHELXT<sup>4</sup> structure solution program using intrinsic phasing and refined with SHELXL<sup>5</sup> using least squares minimisation. All non-hydrogen atoms were refined anisotropically, and the hydrogen atoms were added via a riding model. The crystallographic parameters for **Model\_B1m** are provided in Table 1. The .cif file for this structure has been deposited in the Cambridge Structural Database: CCDC 2182612. These data can be obtained free of charge from the Cambridge Crystallographic Data Centre via [www.ccdc.cam.ac.uk/data\\_request/cif](http://www.ccdc.cam.ac.uk/data_request/cif).

**Table 1.** Selected crystallographic data for the model complex **Model\_B1m**.

	<b>Model_B1m</b>
$\lambda$ (Å)	0.71073
<i>T</i> (K)	93
<b>Crystal system</b>	Monoclinic
<b>Space group</b>	<i>Cc</i>
<i>a</i> (Å)	32.0896(6)
<i>b</i> (Å)	9.7834(2)
<i>c</i> (Å)	20.0973(3)
$\beta$ (°)	96.47(1)
<i>V</i> (Å <sup>3</sup> )	6269.2(2)
<i>Z</i>	8
<i>D</i> <sub>calc</sub> (g cm <sup>-3</sup> )	1.469
<b>Reflections</b>	42157
<b>Unique data</b>	13888
<i>R</i> <sub>int</sub>	0.037
<i>R</i> [ <i>F</i> <sup>2</sup> > 2 $\sigma$ ( <i>F</i> <sup>2</sup> )]	0.053
<i>wR</i> ( <i>F</i> <sup>2</sup> )	0.134
<i>S</i>	1.01
$\rho$ <sub>max</sub> , $\rho$ <sub>min</sub> (eÅ <sup>-3</sup> )	1.51, -0.56

**Detection of CO release.** An acetone suspension of the sample to be analyzed was spin coated on a glass substrate. The weight of the sample was between 150 and 250  $\mu$ g. The sample was placed

in a custom-made chamber with a glass window on the top and irradiated with a 300 W xenon lamp (Asahi Spectra Max-303 equipped with a 300 to 600 nm ultraviolet-visible module and  $\times 1.0$  collimator lens). The light intensity was  $3.7 \text{ mW cm}^{-2}$ . The released CO gas from the CPPs was carried to the CO detector (HALO 3 TM trace gas analyzer from Tiger Optics) by  $\text{N}_2$  flow ( $500 \text{ ml min}^{-1}$  flow rate).

**Stability test in phosphate buffered saline (PBS).** Approximately 1 mg of a given CPP was dispersed in 4 mL of PBS solution. The suspensions were stirred for 24 h at room temperature. Thereafter, the supernatant was separated from the CPP by centrifugation. The concentration of manganese ions in supernatant was determined by Inductively coupled plasma optical emission spectroscopy (ICP-OES). CPPs were washed with water (2 mL) three times and finally dried under vacuum. The difference between before and after stirring in PBS was confirmed by IR spectroscopy.

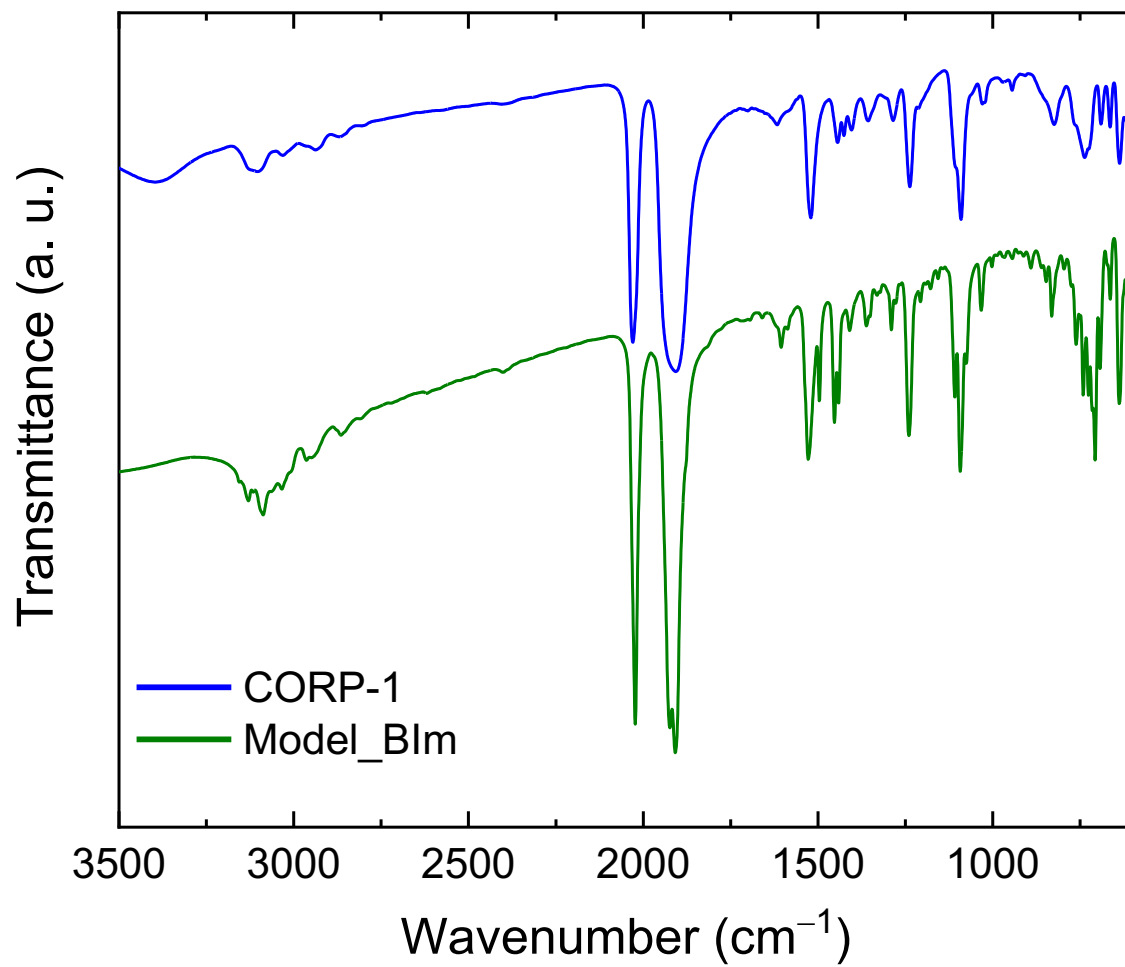


**Fig. S1.** FT-IR spectra for **CORP-1** and **Model\_BIm**.

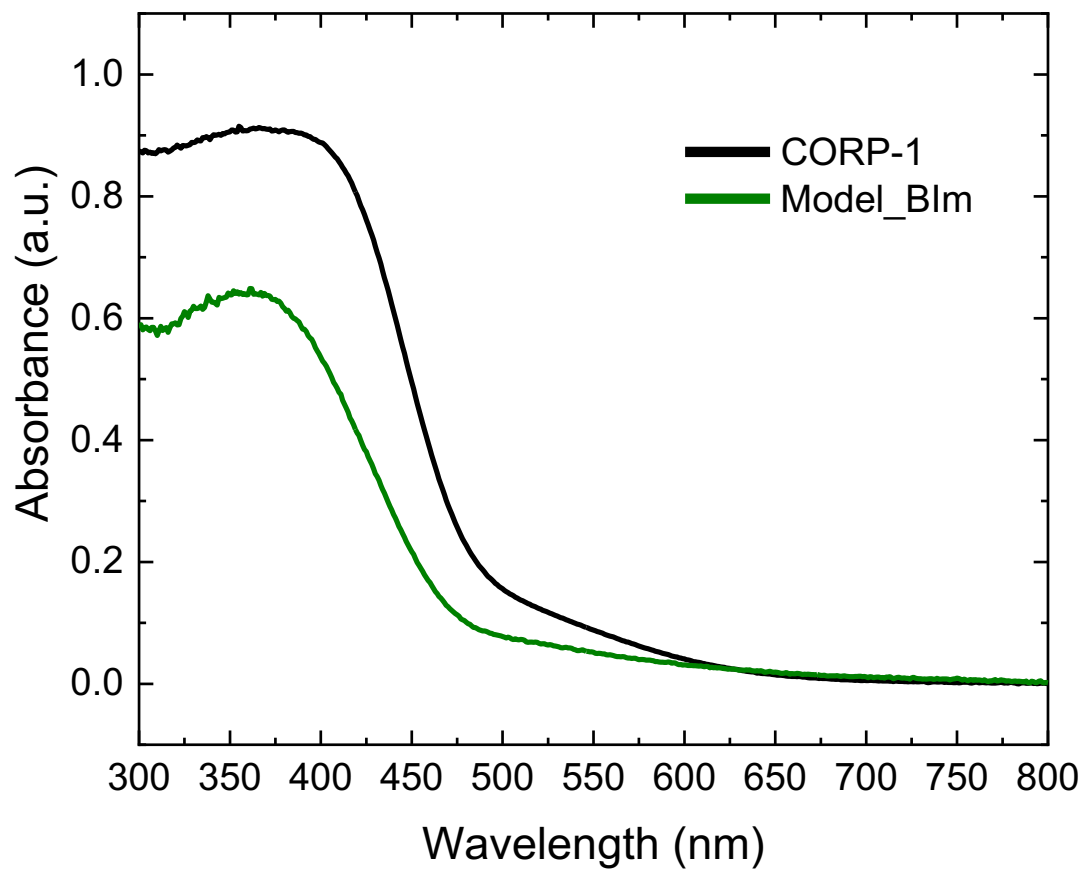


**Fig. S2.** Solid-state UV-vis spectroscopy data for **CORP-1** and **Model\_BIm**.



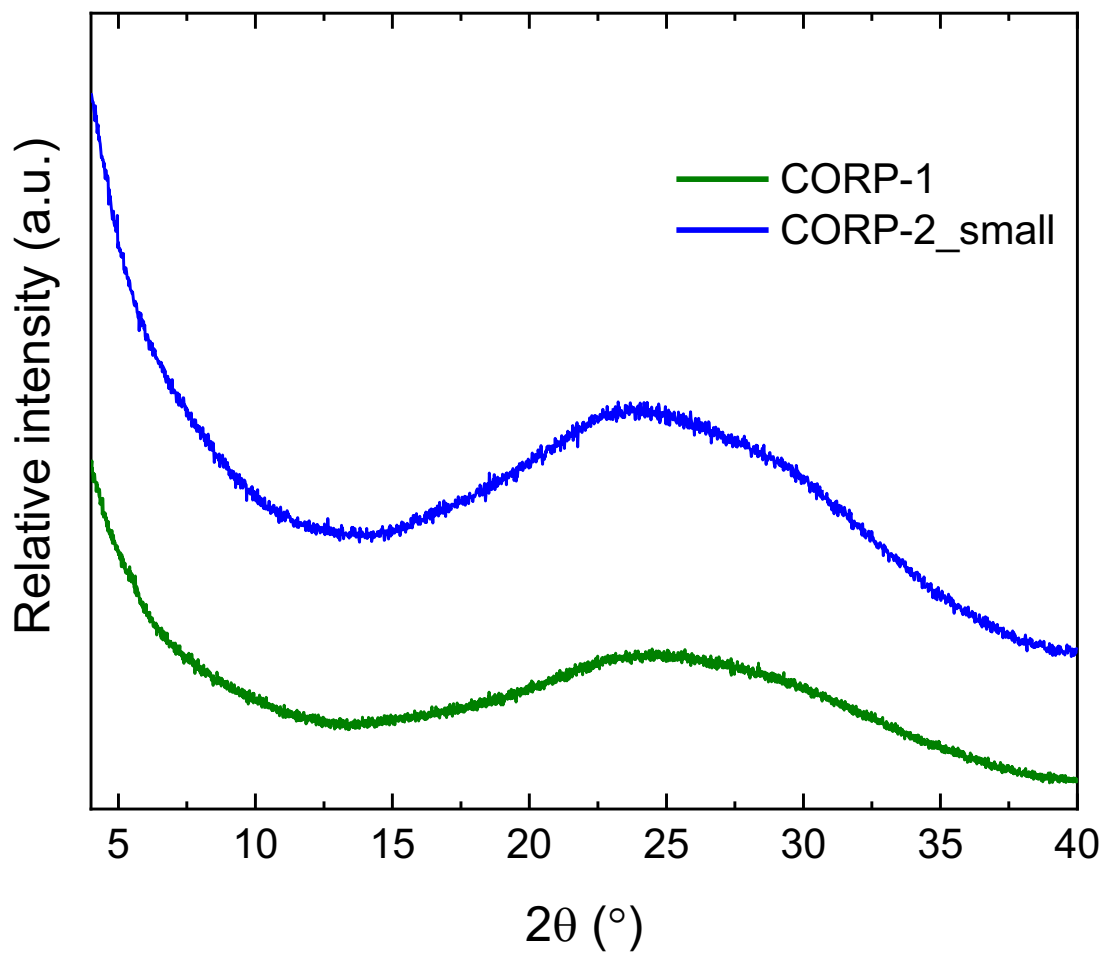


**Fig. S3.** PXRD data for **CORP-1** and **CORP-2\_small**. The diffractograms have been vertically offset for clarity.

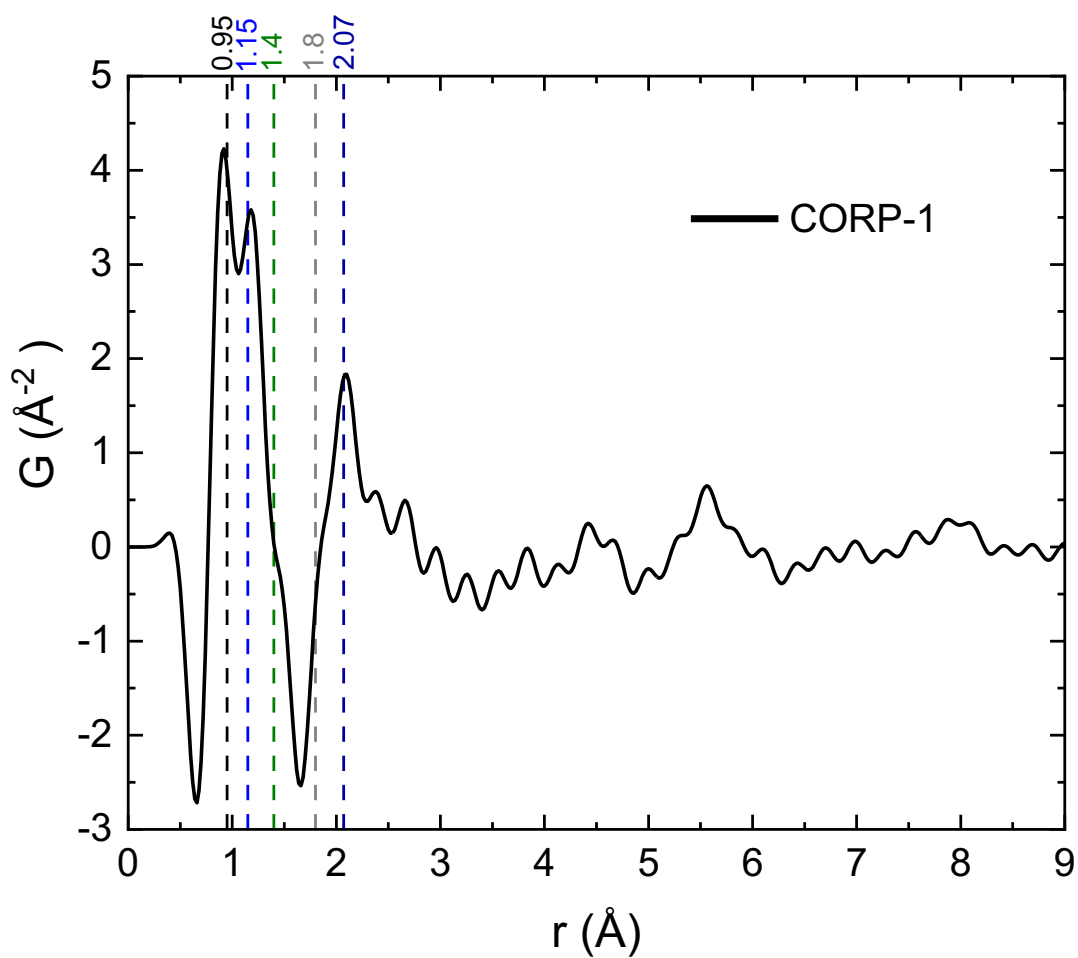
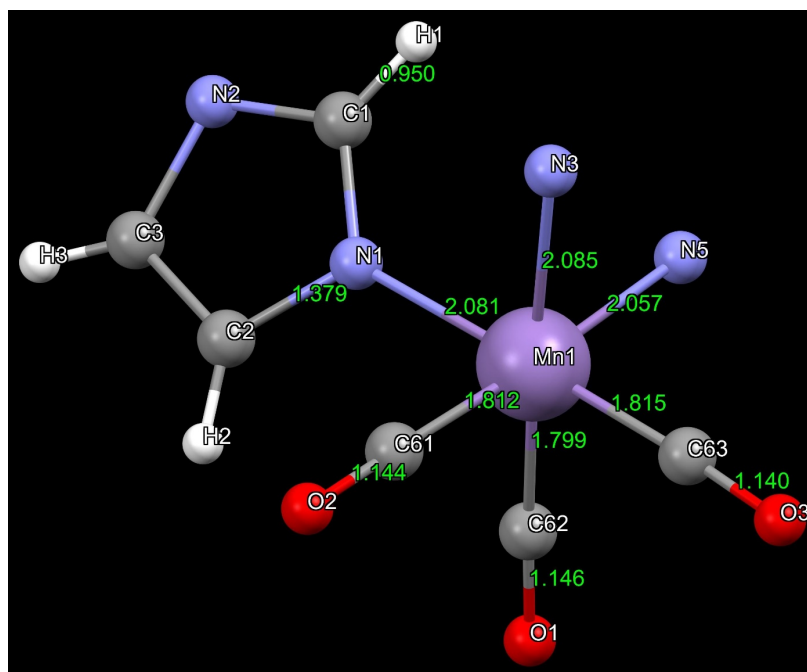


**Fig. S4.** (top) Mercury view of a fragment of **Model\_B1m** and (bottom) PDF data for **CORP-1**.

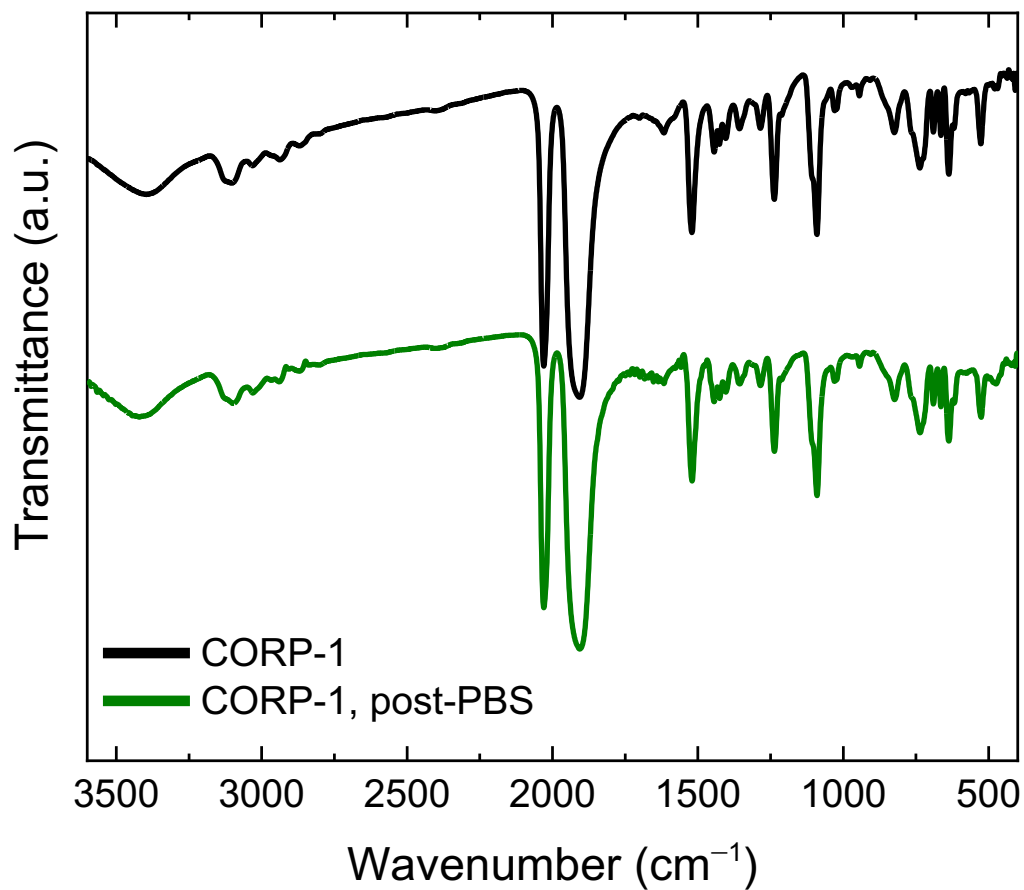


**Fig. S5.** IR spectrum of **CORP-1**, and IR spectrum of **CORP-1** after being stirred in phosphate buffered saline (PBS) for one day.

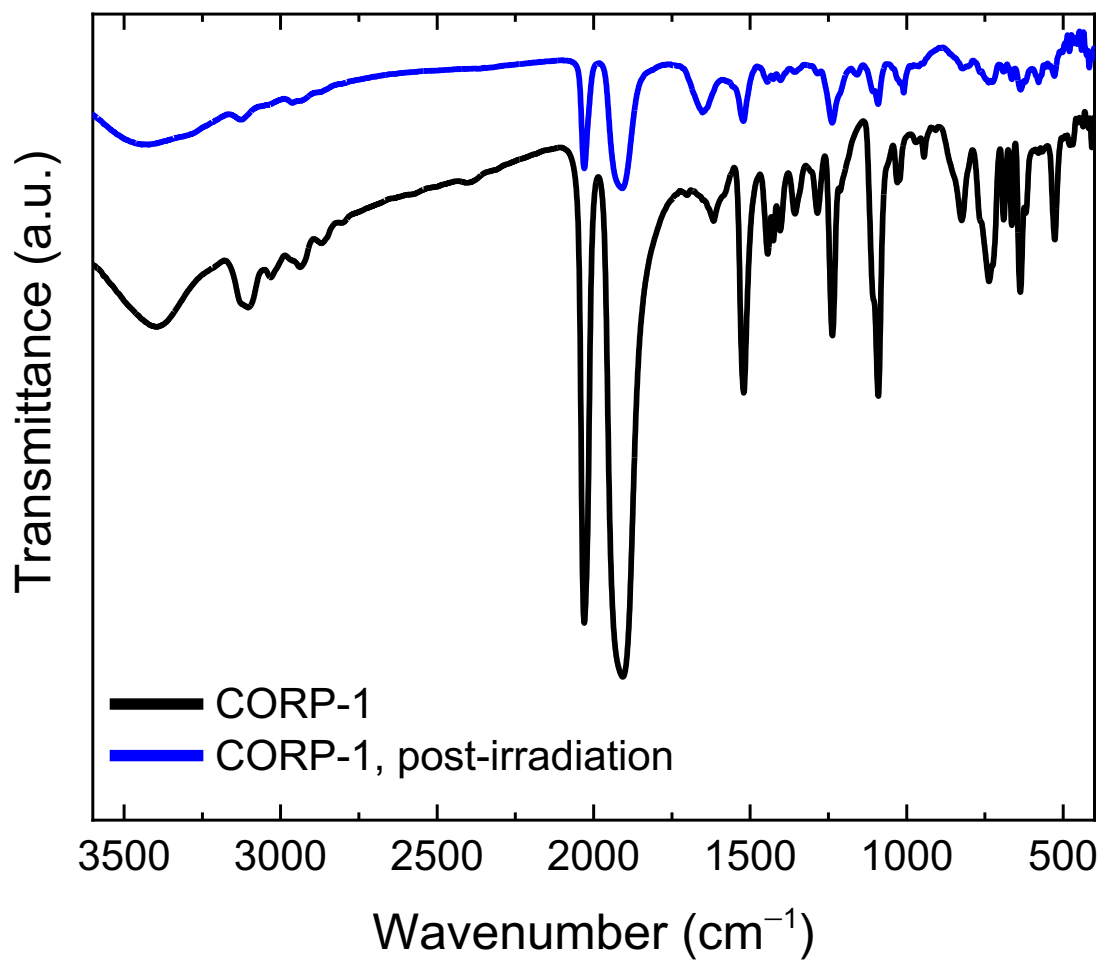


**Fig. S6.** IR spectrum of **CORP-1**, and IR spectrum of **CORP-1** after irradiation for 2 hours.

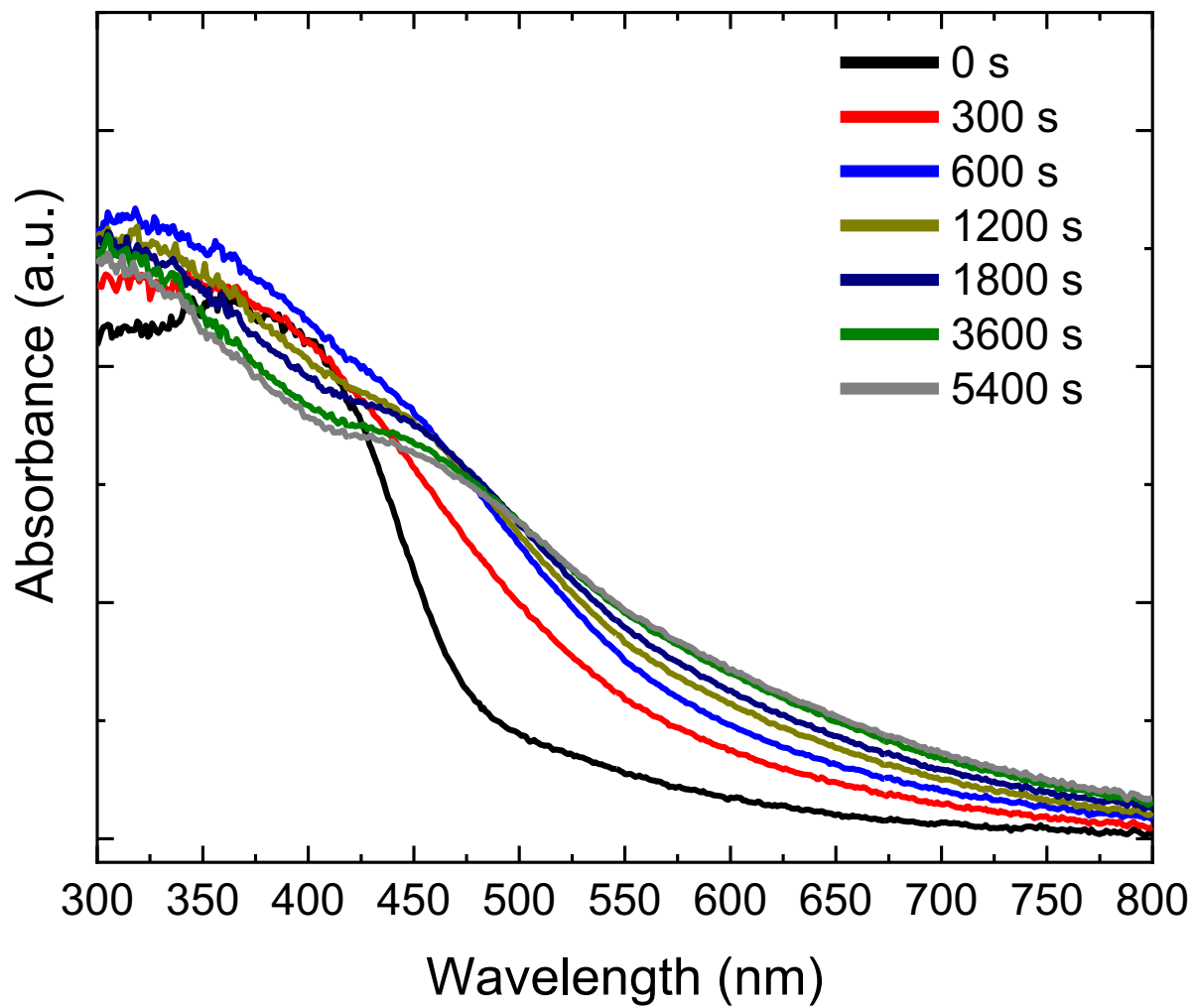


**Fig. S7.** Change in the solid-state UV-vis spectra for **CORP-1** after irradiation for the times shown.

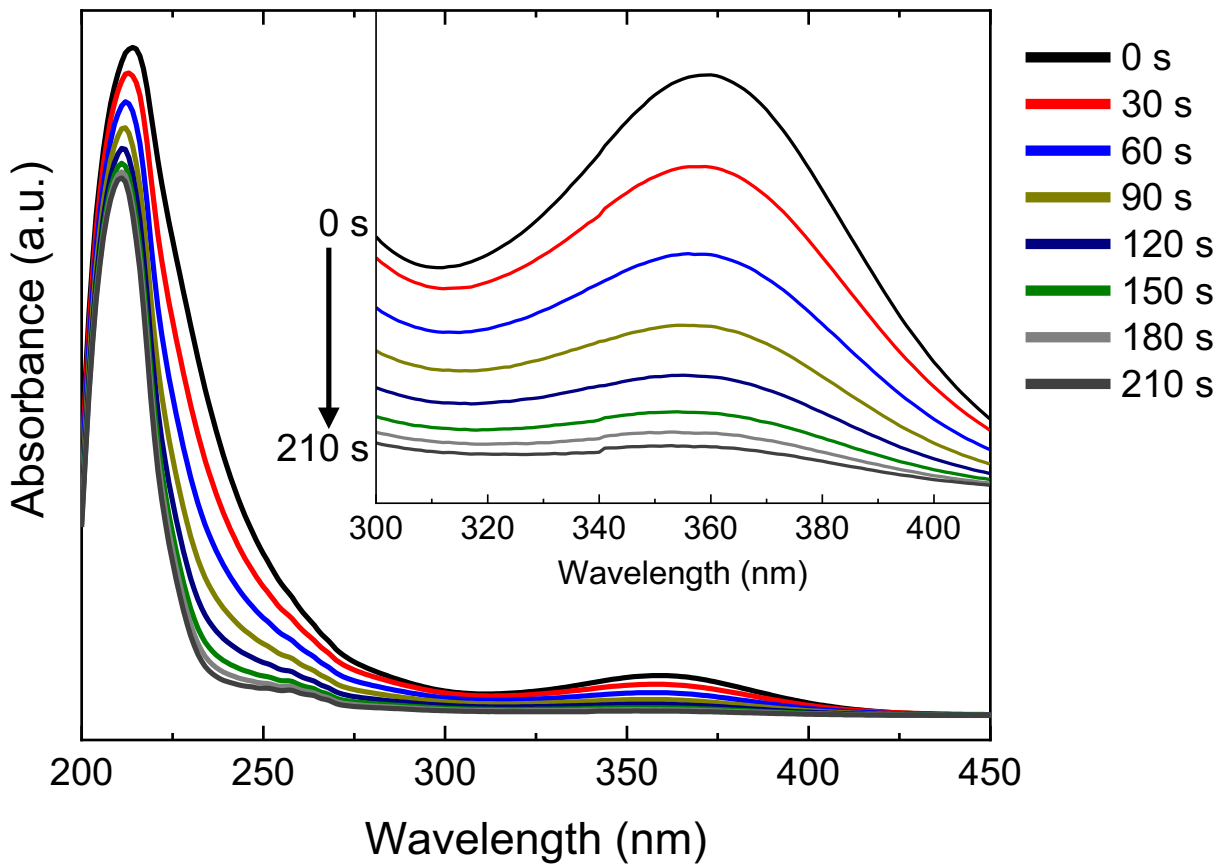


**Fig. S8.** UV-vis spectra of **Model\_BIm** in MeOH solution. The inset shows a magnified view of the spectra between 300 and 410 nm.

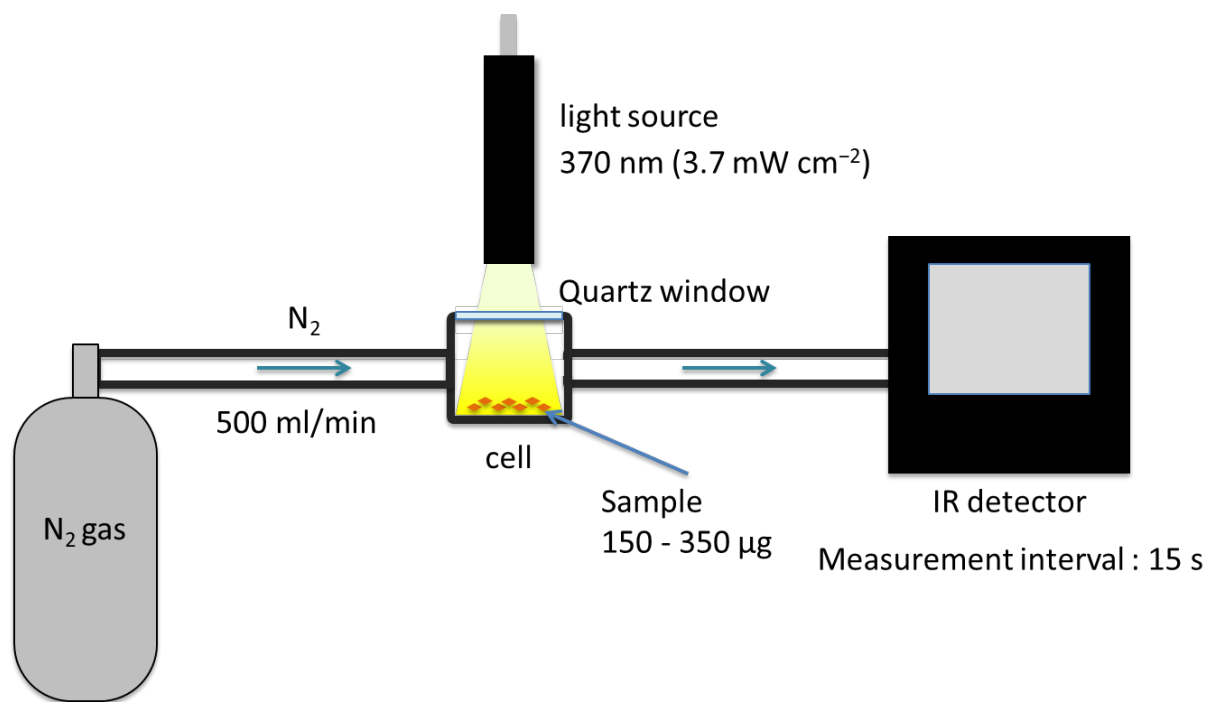


**Fig. S9.** Customised set-up for in-line detection of CO release.

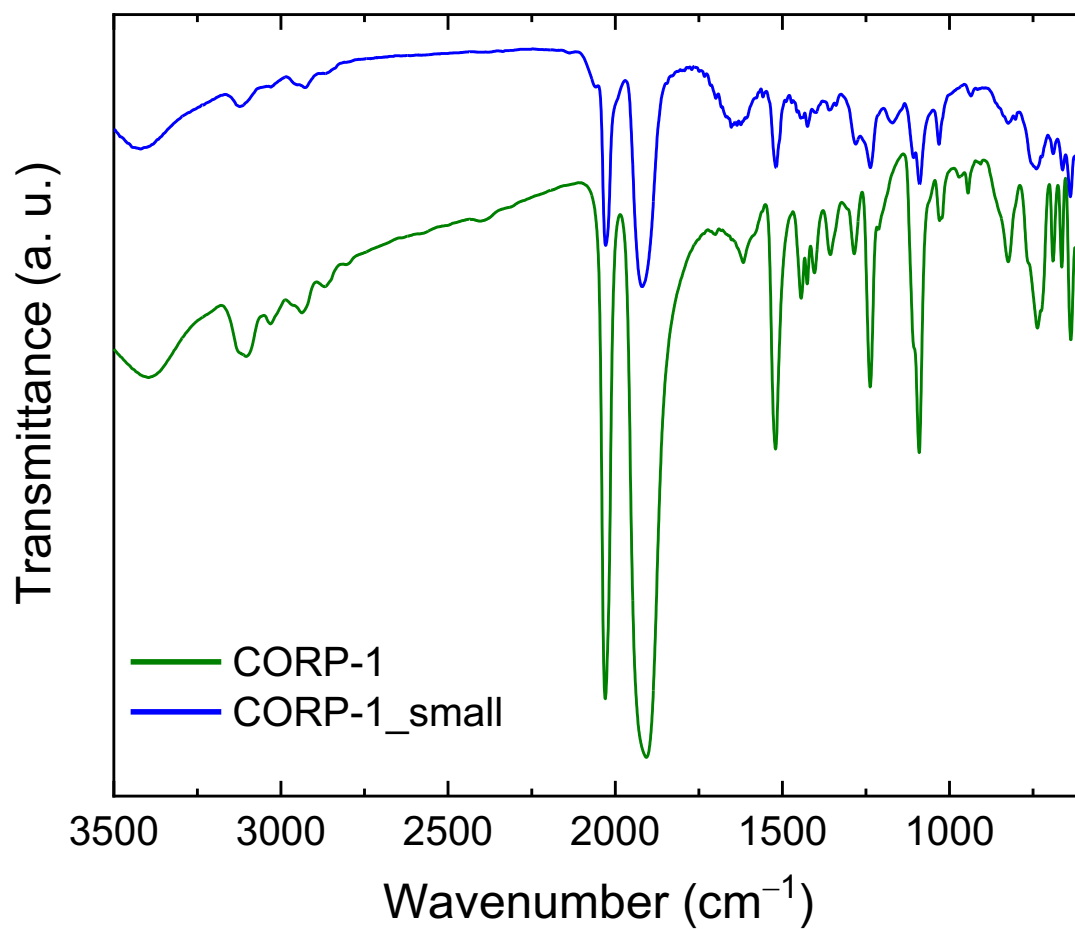


**Fig. S10.** IR spectra for the large and small particles of **CORP-1**.



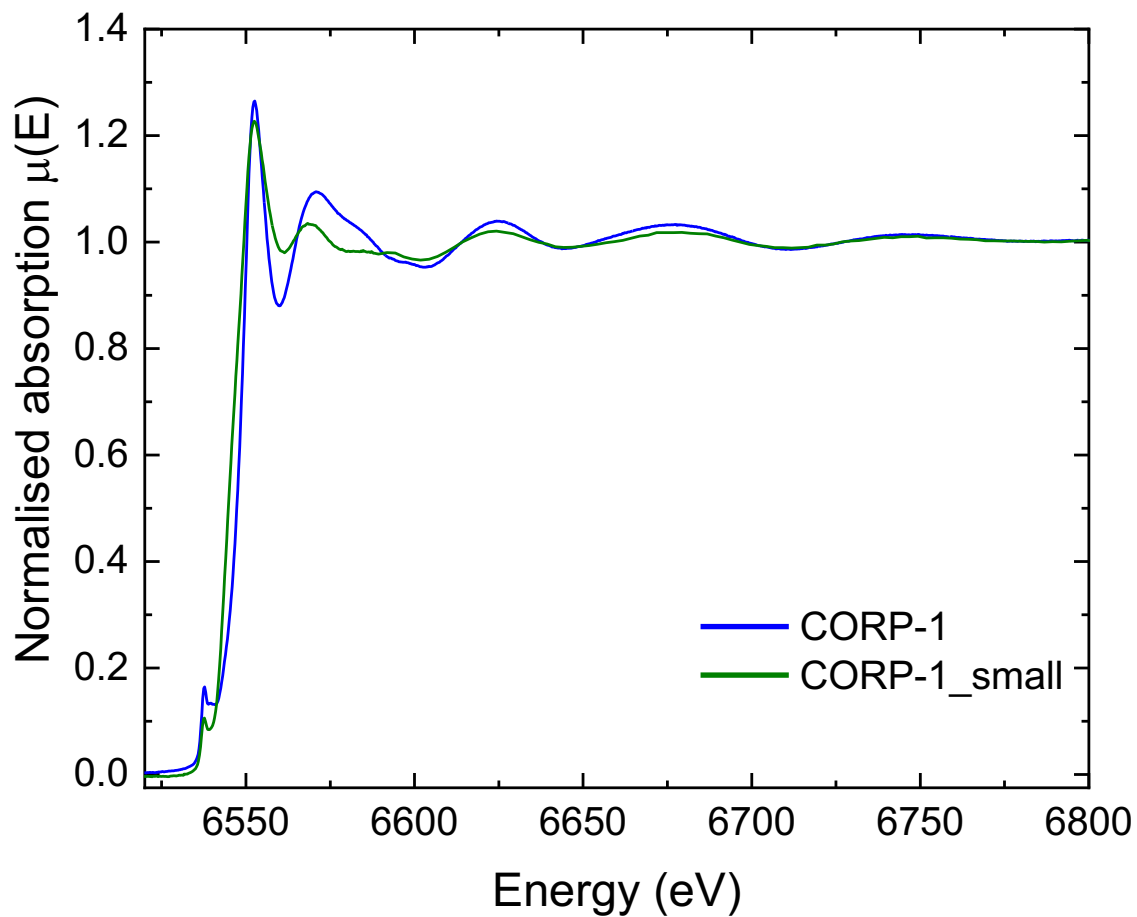


**Fig. S11.** Comparison of the XAFS spectra for the large and small particles of **CORP-1**.

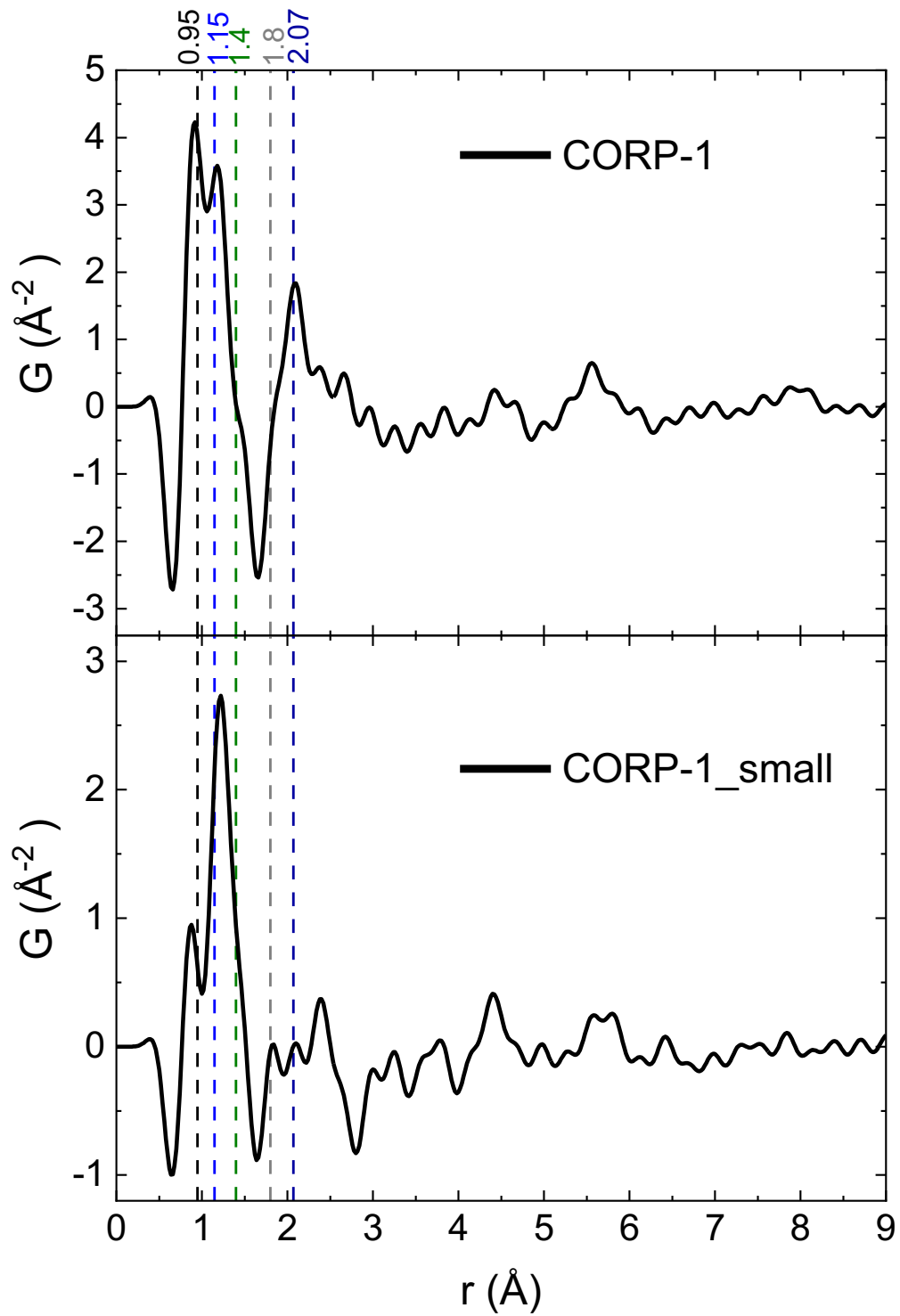


**Fig. S12.** PDF data for **CORP-1** for large particles and small particles.

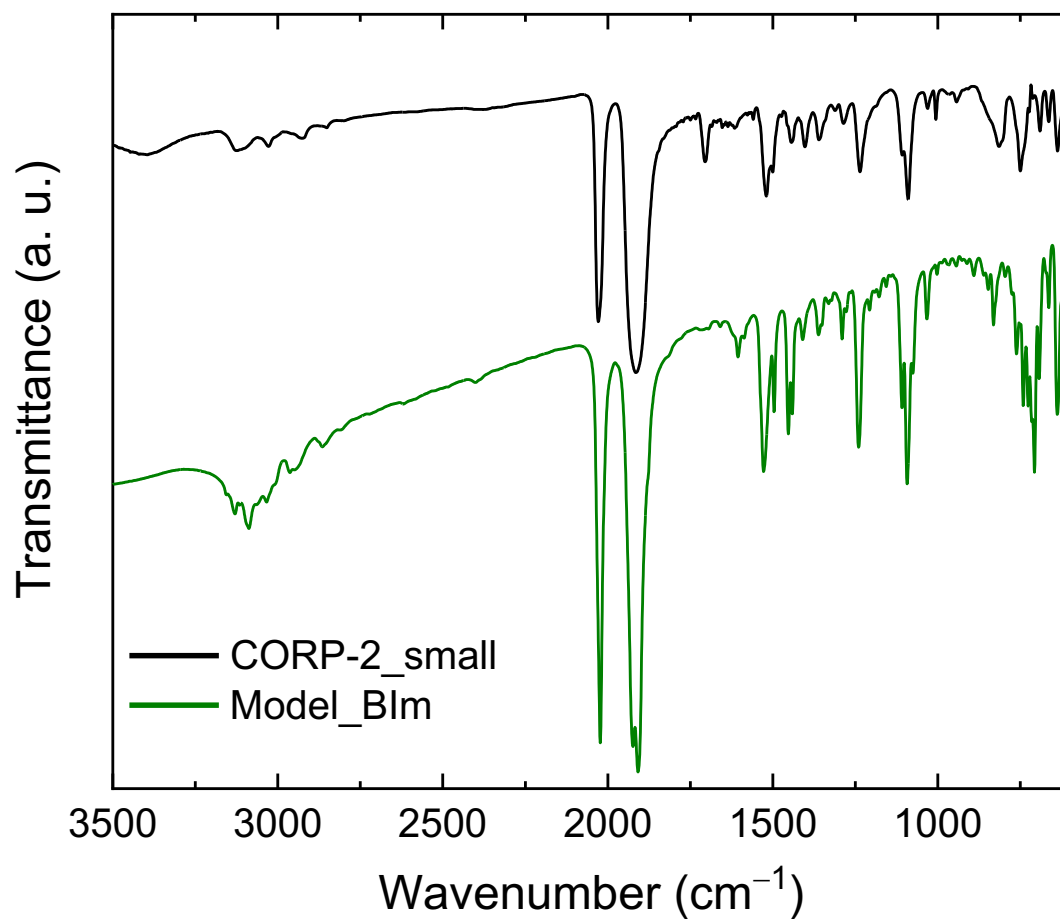


**Fig. S13.** IR spectrum of **CORP-2\_small**, and IR spectrum of **Model\_BIm** for comparison.

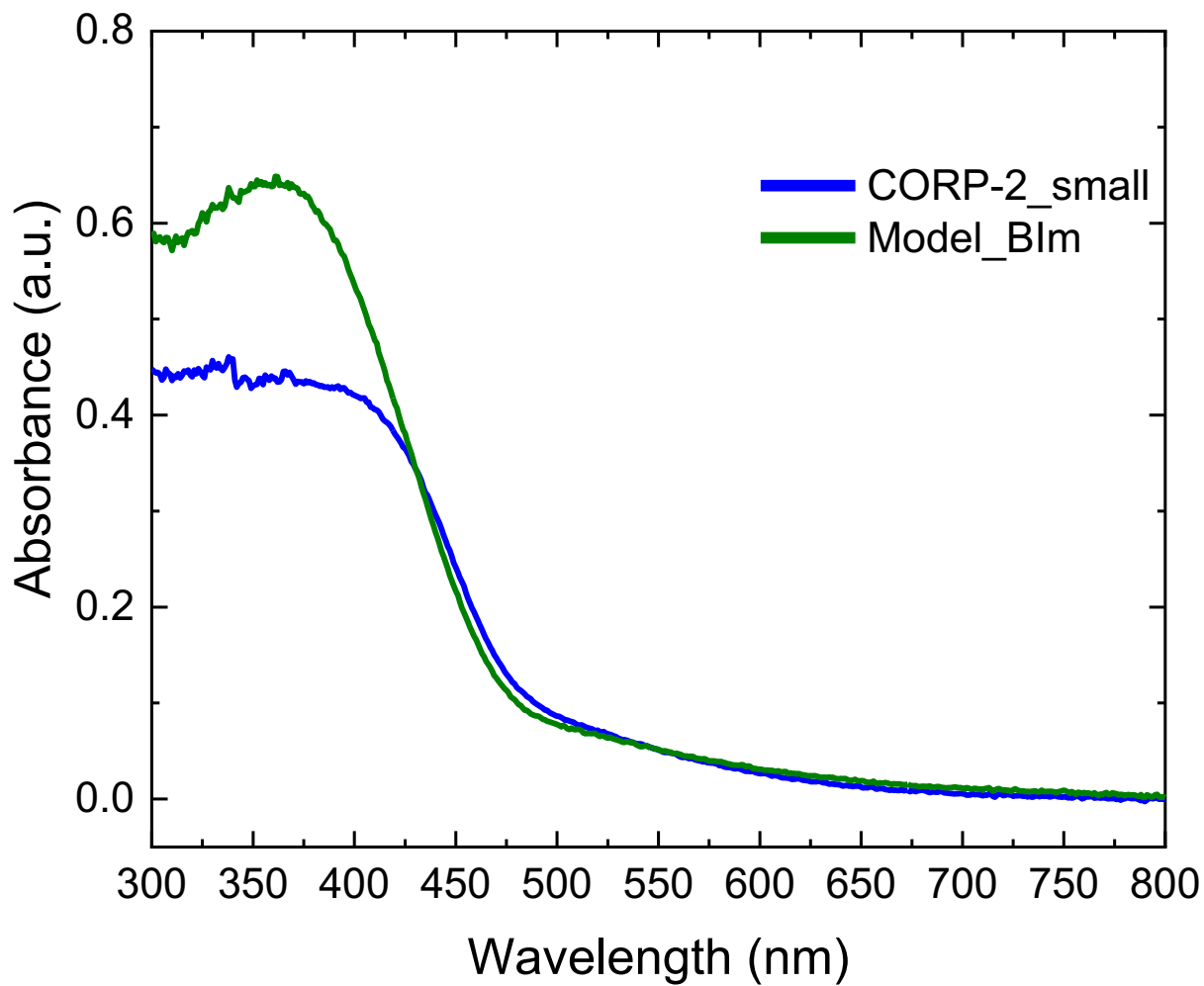


**Fig. S14.** Solid-state UV-vis spectroscopy data for **CORP-2\_small** and **Model\_B1m**.

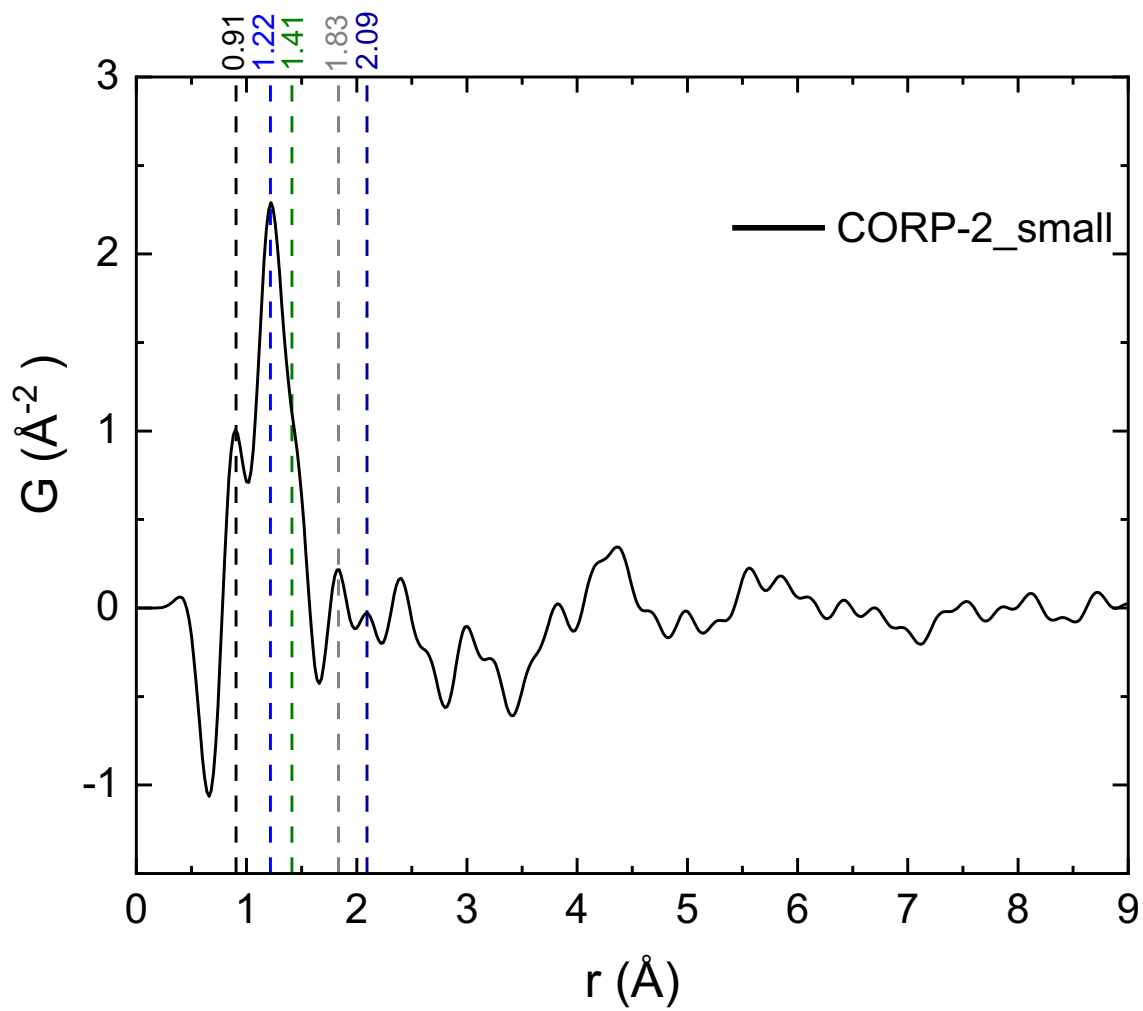


Fig. S15. PDF data for CORP-2\_small.

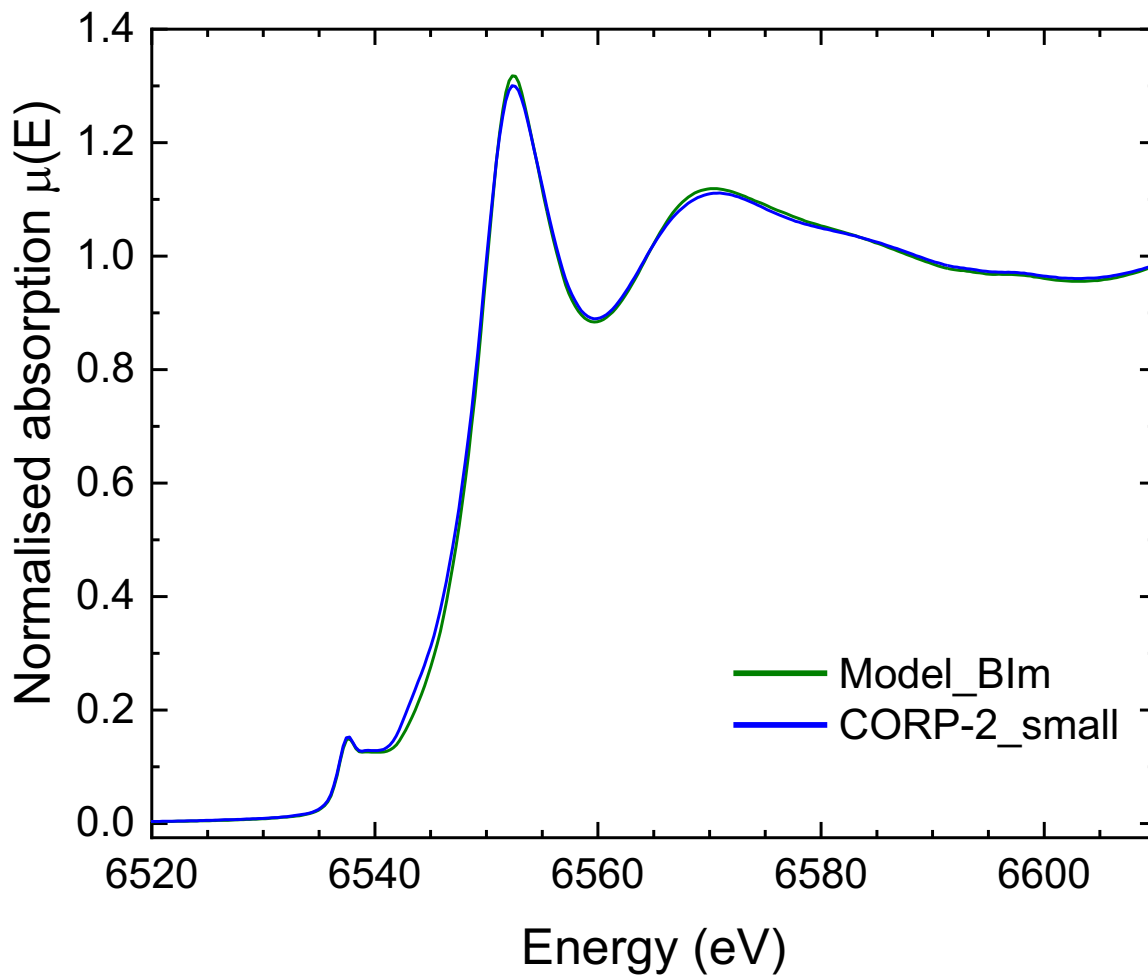


Fig. S16. XAFS spectra for **CORP-2\_small** and **Model\_BIm**.

## References

1. P. K. Dhal, F. H. Arnold, *Macromolecules*, 1992, **25**, 7051-7059.
2. P. Juhas, T. Davis, C. L. Farrow, S. J. L. Billinge, *J. Appl. Cryst.*, 2013, **46**, 560-566.
3. O. V. Dolomanov, L. J. Bourhis, R. J. Gildea, J. A. K. Howard, H. Puschmann, 2009, *J. Appl. Cryst.*, **42**, 339-341.
4. G. M. Sheldrick, 2015, *Acta Cryst.* **A71**, 3-8.
5. G. M. Sheldrick, 2015, *Acta Cryst.* **A71**, 3-8.